Hydrol. Earth Syst. Sci. Discuss., 11, 11335–11368, 2014
www.hydrol-earth-syst-sci-discuss.net/11/11335/2014/
doi:10.5194/hessd-11-11335-2014

Hydrology and Earth System Sciences
Discussions
Open Access

Influence of rain pulse characteristics over intrastorm throughfall hot moments

J. T. Van Stan and T. E. Gay

Department of Geology and Geography, Georgia Southern University, Statesboro, GA, USA

Received: 7 September 2014 – Accepted: 14 September 2014 – Published: 14 October 2014

Correspondence to: J. T. Van Stan (jvanstan@georgiasouthern.edu)

Published by Copernicus Publications on behalf of the European Geosciences Union.

Abstract

Forest canopy alters the amount of rainfall reaching the surface by redistributing it as throughfall. Throughfall is critical to watershed ecological variables (soil moisture, stream water discharge/chemistry, and stormflow pathways) and controlled by canopy structural interactions with meteorological conditions across temporal scales (from seasonal to within-event). This work uses complete linkage cluster analysis to identify intrastorm rain pulses of distinct meteorological conditions (beginning-of-storm and internal-to-storm pulses that are atmospherically dry, moderate, or wet), relates each cluster to intrastorm throughfall responses, then applies multiple correspondence analyses (MCAs) to a range of meteorological thresholds (median intensity, coefficient of variation (CV) of intensity, mean wind-driven droplet inclination angle, and CV of wind speed) for identification of interacting storm conditions corresponding to hot moments in throughfall generation ($\geq 80\,\%$ of rainfall). Equalling/exceeding rain intensity thresholds (median and CV) corresponded with throughfall hot moments across all rain pulse types. Under these intensity conditions, two wind mechanisms produced significant correspondences: (1) high wind-driven droplet inclination angles under steady wind increased surface wetting; and (2) sporadic winds shook entrained droplets from surfaces. Correspondences with these threshold conditions were greatest for pulses of moderate vapour pressure deficit (VPD), but weakest under high VPD. Weaker correspondences between throughfall hot moments and meteorological thresholds for high VPD pulses may be because canopy structures were not included in the MCA. In that vein, strongest meteorological threshold correspondences to throughfall hot moments at our site may be a function of heavy *T. usneoides* coverage. Future applications of MCA within other forests are, therefore, recommended to characterize how throughfall hot moments may be affected along drainage paths dependent on different structures (leaves, twigs, branches, etc.).

1 Introduction

The extent and type of forest cover can exert significant influence over watershed hydrologic processes through the physiological (transpiration) and physical partitioning of meteoric water (Bachmair and Weiler, 2011; Carlyle-Moses and Gash, 2011; Kumagai, 2011; Tanaka, 2011). Physically, when rainfall contacts canopy elements (leaves, branches, epiphytes, etc.) it either: (1) is stored and evaporated (as interception loss), (2) gets diverted along the branch and trunk structures to the soils surrounding the main stem (as stemflow), or (3) penetrates the gaps and drips from the canopy (as throughfall). Of these physical rainfall partitions, throughfall represents the greatest percentage across all measured forest types and climates: 70–90 % (Levia and Frost, 2006; Levia et al., 2011). Spatiotemporal patterns in throughfall inputs are highly heterogeneous across and within storms, leading to "hot" and "cold" spots and moments of water receipt to forest soils (Stout and McMahon, 1961; Keim et al., 2005; Zimmermann et al., 2007; Fathizadeh et al., 2014). Throughfall receipt at the soil surface has been linked to critical watershed-scale ecological variables: soil moisture/chemistry (Manderscheid and Matzner, 1995), stream water discharge and chemistry (James and Roulet, 2006; Inamdar and Mitchell, 2007; Chaves et al., 2008), and even watershed stormflow pathways (Singh et al., 2014). Thus, understanding and predicting throughfall spatiotemporal patterns in forests is of critical import to improved characterization of hydrologic and biogeochemical cycling in wooded watersheds (Levia et al., 2011).

Much past research regarding throughfall spatiotemporal patterns has focused on the spatial configuration of hot and cold spots, and its temporal persistence (e.g., Keim et al., 2005; Shachnovich et al., 2008; Zimmermann et al., 2009; Guswa and Spence, 2012; Fathizadeh et al., 2014). An even greater body of literature has identified meteorological and stand structural controls over throughfall temporal variability (see reviews by Levia and Frost, 2006; Levia et al., 2011), yet research regarding interactive effects of these two conditions is needed (Pypker et al., 2011).

Generally for meteorological influences, throughfall has been shown to increase with rainfall amount and intensity (Helvey and Patric, 1965; Návar and Bryan, 1990; Crockford and Richardson, 2000; Murakami, 2006), while wind conditions can enhance canopy capture and diversion of rain to throughfall in individual canopies (Herwitz and Slye, 1992, 1995) or, when canopy shaking is induced, wind can prevent rainwater coalescence on canopy elements, thereby increasing throughfall drip (Calder, 1996; Hall, 2003; Nanko et al., 2006). But, under what combination of these meteorological conditions, or combination of thresholds in these conditions, will a forest canopy permit the greatest or least throughfall generation? Further, these meteorological-throughfall interactions are primarily based on storm-level data, which lump multiple intrastorm rain-throughfall pulses together and neglect that these pulses may produce contrasting rain-throughfall responses.

In terms of canopy structural impacts on throughfall generation, leaf shape, configuration, and surface hydrophobicity can alter water storage and, therefore, throughfall amount (Horton, 1919; Keim et al., 2006; Holder, 2013; Rosado and Holder, 2013). Bark structures and branching architecture may also affect throughfall generation by changing water storage (Herwitz, 1985), yet can further amend throughfall by geometric branch orientation impacting the interchange between drip and stemflow drainage (Herwitz, 1987; André et al., 2008). Another factor able to increase canopy water storage at the expense of throughfall is epiphyte coverage (Hölscher et al., 2004; Pypker et al., 2006a, b; Köhler et al., 2007; Van Stan et al., 2014). However, despite epiphytes' capability to store water in excess of 1000 % of their dry weight, this storage is reduced in situ as epiphytes are not typically able to dry completely between storms (Hölscher et al., 2004; Pypker et al., 2006b, 2011). Yet, when saturated, stable epiphyte structures may be able to generate hot moments/spots of throughfall generation depending on meteorological conditions (Zimmermann et al., 2007). Along the southeastern US coastline, stable epiphyte structures – *Tillandsia usneoides* L. (Spanish moss) – are prevalent throughout maritime forests (Schlesinger and Marks, 1977; Husk et al., 2004; Van Stan et al., 2014). How do throughfall pulses

HESSD
11, 11335–11368, 2014

Rain pulse influence over throughfall hot moments

J. T. Van Stan and T. E. Gay

respond to rainfall pulses occurring under contrasting meteorological conditions for forests of heavy *T. usneoides* coverage? Moreover, is there a cocktail of meteorological conditions under which throughfall amounts beneath *T. usneoides*-covered forests are enhanced?

Our study seeks to investigate such questions at the intersection of forest structural and meteorological conditions by: (1) using intrastorm hydrometeorological monitoring and complete-linkage cluster analysis to identify distinct categories of intrastorm rainfall pulses, (2) examine whether these rain pulse categories differentially affect within-event throughfall generation; and (3) apply Multiple Correspondence Analysis (MCA) to detect threshold meteorological conditions (rainfall inclination angles, wind speed variability, rain intensity, and variability in rain intensity) conducive to intrastorm hot moments in canopy throughfall generation (≥ 80 % of rainfall) for all pulses and individual pulse categories. We hypothesized that intrastorm rain-throughfall pulses will: (1) generally break into beginning or internal storm pulses under dry or wet atmospheric conditions, (2) produce significantly different throughfall amounts, (3) generate hot moments in throughfall generation (≥ 80 % of rainfall) under consistently high wind, low vapour pressure deficit (VPD), and high rain intensity conditions across the categories as this will minimize the epiphyte's storage effect.

2 Materials and methods

2.1 Study site description

St. Catherine's Island (SCI) is situated along the Georgia coast (Fig. 1) in the subtropical climate (Köppen *Cfa*) zone, where temperatures rarely dip below freezing during the winter (GA-DNR-WRD, 2013). 30 year mean annual rainfall is approximately 950 mm yr^{-1}, but can be as low as 750 mm yr^{-1} or high as 1200 mm yr^{-1} (GA Office of the State Climatologist, 2012). In summer, rainfall is dominated by convective thunderstorms due to the Bermuda high-pressure system, producing mean 30 year

Discussion Paper | Discussion Paper | Discussion Paper | Discussion Paper |

HESSD

11, 11335–11368, 2014

Rain pulse influence over throughfall hot moments

J. T. Van Stan and T. E. Gay

rainfall ranging from 65 to 150 mm month^{-1} between May and August. Winter rainfall is sparser (0–100 mm month^{-1} between November and February) as the Bermuda high can drive fronts northward. The biometeorological monitoring site is in a *Quercus virginiana* Mill. (southern live oak) forest (Fig. 1) where, according to the National Resources Conservation Service (NRCS) Web Soil Survey, soils beneath are mainly Foxworth series, with low slope (0–3 %) and deep, moderately well-drained fine sands with high permeability (K_{sat} = 15–51 cm h^{-1}). Stand density is 278 trees ha^{-1}, containing 48.7 m^2 of basal area ha^{-1}. *Quercus virginiana* Mill. (southern live oak) is the dominant canopy cover in this plot (58 % of species), followed by a variety of other species at comparatively low proportions – 18 % *Carya glabra* Miller (pignut hickory), 18 % *Pinus taeda* L. (loblolly pine), 3 % *Juniperus virginiana* L. (eastern red cedar), and 3 % *Sabal palmetto* (Walt.) Lodd. (sabal palm) – with small diameters at breast height (dbh: range from < 10 cm to 20 cm). In the 1 ha plot, *Q. virginiana* accounts for 85.7 % of trees over 20 cm dbh and has a mean dbh of 36.6 cm ± 13.1 cm standard deviation. This maritime *Q. virginiana* forest hosts substantial *T. usneoides* cover: 4 convex spherical densiometer measurements (north, south, east, and west) over 15 plots randomly throughout the 1 ha site estimate *T. usneoides* coverage at 17.1 % of the canopy area ±6.5 % standard deviation – and a maximum of 32.3 % of the canopy area. This is a striking abundance of epiphyte cover as similar densiometer measurements focusing, more conventionally, on canopy cover percentage estimate total canopy coverage at 68.8 %, which reveals that *T. usneoides*-covered canopy represents nearly one-quarter of the total cover at this plot on SCI.

2.2 Hydrometeorological monitoring

Hydrometeorological monitoring at SCI began in September 2013 and conclusion of data collection for this analysis was on 31 July 2014. Meteorological conditions were monitored continuously (at a 5 min interval) using Climatronics Corp. instruments (Bohemia, New York, USA), including a: 20.3 cm dual-chambered tipping bucket rain gauge (model 100097-G0-H0) for rainfall, wind speed/direction sensor (model 102870) installed 2 m above ground elevation, and relative humidity/temperature sensor outfitted with a naturally-aspirated radiation shield (model 102798). All meteorological monitoring instruments were interfaced to a single Campbell Scientific CR1000 datalogger, and the station was situated in the open, about 1 km westward of the throughfall monitoring equipment. Vapour pressure deficit (VPD) was computed from temperature and relative humidity values every 5 min. Rainfall inclination angles were calculated every 5 min per the following process: (1) relate intensity to median droplet size using Law and Parsons' (1943) formula, then determine terminal fall velocity of the median droplet size (Gunn and Kinzer, 1949) and, finally, the inclination angle is the arctangent of the ratio between mean wind speed and terminal fall velocity (as described in further detail by Herwitz and Slye, 1995 and Van Stan et al., 2011). Wind run (km) was also computed at the 5 min interval as the product of mean wind speed ($km\,h^{-1}$) and duration (h). Intrastorm throughfall monitoring was done using seven 3.048 m long and 10.16 cm diameter PVC troughs oriented at a moderate slope, with a 5.08 cm slot cut lengthwise to accept and drain throughfall from each trough to a Texas Electronics (Dallas, Texas, USA) TR-525I tipping bucket gauge. Each trough-tipping bucket assembly was arranged randomly in place and direction within a 50 m × 50 m subplot and interfaced with a Campbell Scientific CR1000 datalogger set to record observations at 5 min intervals. Total 5 min throughfall observations were computed as the sum of all gauges (mL) divided by the sum of their area (cm^2). PVC trough angles were measured directly with a digital clinometer to correct trough area calculations. It is important to note that, per the manual, a TR-525I gauge is accurate (±1 %) only up to 50 $mm\,h^{-1}$ at the standard 186.1 cm^2 funnel area (verified with field calibration). By expanding the area for each TR-525I gauge nearly 8 times with the PVC troughs, this lowers the gauge ±1 % accuracy range proportionally, limiting rainfall intensities to ≤ 6.25 $mm\,h^{-1}$ in theory. Field calibration showed the trough-gauge assembly to be ±5 % accurate at rainfall intensities ≤ 10 $mm\,h^{-1}$, which was acceptable

HESSD
11, 11335–11368, 2014

for our study site as the maximum throughfall intensity measured during the monitoring period was 6.15 mm h^{-1}.

2.3 Pulse delineation and defining a throughfall "hot moment"

Using discrete storm classification criteria – any measureable rainfall preceded by a minimum 8 h antecedent dry period (ADP) – 56 storms without clogs or gauge malfunctions were collected during the hydrometeorological monitoring period. Yet, this study seeks to characterize and explore the temporal dynamics of individual rainfall-throughfall pulses within storm events themselves. Rainfall pulses were, thus, separated from each discrete event when the following conditions were met: (i) any continuous rainfall ≥ 10 min in duration with (ii) a minimum antecedent dry period of 30 min, and (iii) a corresponding identifiable pulse of throughfall. 41 % (23) of the discretely-defined events consisted of one rainfall-throughfall pulse, and the mean number of pulses per discrete storm was approximately 3. Of the total intrastorm rain pulses, 69 were included in the following analyses. Intrastorm rain pulses not included in the analyses were those with throughfall responses too close together for adequate separation (violating condition 3, above).

Defining hot moments in ecosystem processes has evolved to include a diversity of phenomena (Bundt et al., 2001; McClain et al., 2003; Vidon et al., 2010; Andrews et al., 2011; Liengaard et al., 2014), most notably based on whether the process being considered is temporarily and significantly elevating (i) reaction rates or (ii) transport of materials (Vidon et al., 2010). Hot moments of elevated reaction rate may, for instance, focus on time periods where nutrient pools are consumed, augmented, or altered in quality or chemical character. Alternatively, periods of elevated solute or water flux to an ecosystem compartment during storm events may be considered transport-driven hot moments. This study seeks to identify transport-driven hot moments during storm events (specifically, enhanced translation of rainfall pulses into throughfall pulses by forest canopies) and characterize the combination of meteorological thresholds under which these throughfall transport hot moments occur. As past research regarding

HESSD
11, 11335–11368, 2014

transport-driven hot moments have used percentages compared to the norm (e.g., Vidon et al., 2010; Andrews et al., 2011), we will define throughfall hot moments as those whose percentage of incident rainfall are much greater than the average observed for the canopy being monitored (73 %). The degree to which intrastorm throughfall responses to rain pulses are "hot" compared to this mean value is, to some extent, relative. But, as there is an upward bound of 100 %, and there is only 27 % between the mean and this upward bound, we chose to consider the lower threshold of any throughfall transport hot moment to be 80 % of the corresponding rain pulse.

2.4 Statistical analyses

Non-uniformly distributed rainfall characteristics necessitated hierarchical cluster analysis for indentifying unique rainfall pulse groupings (Tan et al., 2005). To avoid or minimize variable redundancy, the cluster analysis was performed on rain amount, CV of intensity, wind run, VPD, and ADP. Under the single linkage amalgamation rule, clusters fell prey to chaining. As a result, the complete linkage amalgamation rule was applied. Then, clusters were selected from the resulting hierarchical tree plot and associated statistical measures. Throughfall amount, percentage of rainfall, and intensity data were skewed and, since throughfall events are not dependent on previous throughfall events, non-parametric statistical comparisons of throughfall among the rainfall pulse clusters were performed via Kruskal Wallis ANalysis Of VAriance (ANOVA) tests. Then, to identify threshold meteorological conditions under which throughfall generation (as a percentage of rainfall) is maximized (throughfall "hot moments"), Multiple Correspondence Analyses (MCAs) were applied to all storm pulses and each rainfall pulse cluster (for a more detailed explanation of MCA, readers are referred to Van Stan et al., 2011). In this case, MCA required binary-coded threshold values for (i) when throughfall amounts are considered high relative to the norm (we chose ≥ 80 % of rainfall for this site), and (ii) chosen 5 min meteorological conditions: rainfall inclination angle, rain intensity, and intermittency expressed as CV of wind speed and intensity. Threshold values were chosen through an optimization process seeking the best combination of a range of meteorological condition thresholds yielding the highest overall correspondence (or statistical inertia) for two dimensions when using all pulses, and one dimension when using individual pulse cluster data. Potential thresholds for: rainfall inclination angle were 15, 17, 19, 21, 23, and 25° ; intensity were 0.5, 0.6, 0.7, 0.8, and 0.9 mm 5 min^{-1}; CV intensity were 0.75, 1.0, 1.25, and 1.5 mm 5 min^{-1}; and CV wind were 0.6, 0.7, 0.8, 0.9, and 1.0 m s^{-1}. The optimization process yielded maximum inertia values for a rainfall inclination angle ≥ 17° (A:1 vs. A:0), intensity ≥ 0.6 mm 5 min^{-1} (I:1 vs. I:0), CV 5 min wind speed ≥ 0.6 m s^{-1} (CVW:1 vs. CVW:0), and a CV intensity ≥ 1 mm 5 min^{-1} (CVI:1 vs. CVI:0). Dimension %-inertia values all met the "rule of 1" (e.g., Preisendorfer et al., 1981), where correspondence attributed to the dimension must account for at least more than the %-inertia that could be attributed by any individual variable (e.g., 5 total variables including the throughfall threshold = 1/5 = 20 % of inertia).

3 Results

3.1 Rainfall pulse clustering and characteristics

Total rainfall produced by the pulses included in this analysis was 552.8 mm (Table 1), which represents nearly 70 % of the approximately 800 mm total annual rainfall for 2013–2014 at SCI. Median rainfall amount of all pulses was 2.7 mm (Table 1), with the greatest rainfall pulse producing 54.2 mm of low intensity over 15 h (intensity = 3.46 mm h^{-1}). Median rain intensity for all pulses was 0.8 mm h^{-1}, with a standard error of 0.28 mm h^{-1}. The intensities of the rain pulses did not exceed 6.74 mm h^{-1}. For all rain pulses, wind speed and run medians were 1.7 m s^{-1} and 21 km (Table 1), with maximums of 4.9 m s^{-1} and 428 km, respectively. Measures of event intermittency included CV rainfall intensity and wind speed. Median CV rainfall intensity for all storm pulses was 0.8 mm 5 min^{-1} with a low standard error (Table 1), yet CV wind speed median was even lower (0.4 m s^{-1}) with an even lower standard error (0.07). VPD

HESSD
11, 11335–11368, 2014

median for all rain pulses was less than 100 Pa, which pairs well with the median ADP for this group being only 4 h (Table 1).

Complete linkage clustering revealed four distinct groups of rainfall pulses, for which select storm conditions (those with the greatest variability among clusters) are provided (Table 1). Since the largest number of rainfall pulses are cluster 3 (29 of 69), it is no surprise that it accounts for the largest proportion of total rainfall (Table 1). Rainfall pulse clusters 2 and 4 were roughly equivalent in total rainfall amounts, despite cluster 4 having a greater number of observations (Table 1). Cluster 1 rainfall characteristics indicate that these rainfall pulses are typically low magnitude storms (lowest median rain amount of all clusters) of steady intensity (lowest median CV intensity of all clusters), low wind speed (lowest median wind run of all clusters) and high atmospheric dryness (highest median VPD of all clusters) (Table 1). Having the highest median ADP by nearly an order of magnitude, cluster 1 also represents those rain pulses that begin after long dry periods – which further explain the high median VPD (Table 1). Rainfall characteristics for pulse cluster 2 showed moderate magnitude storms of the highest median CV intensity for all clusters and second-highest median VPD (Table 1). Although median wind runs for rain pulse cluster 2 were second-lowest of all clusters, the standard error in wind is so large (largest of all clusters) that wind does not appear to be an important determinant of this type of rain pulse (Table 1). Short ADPs for cluster 2 indicate these rain pulses occur sometime after the initial pulse of discrete storm events (Table 1).

The largest cluster, cluster 3, also produced the largest median rainfall magnitude and wind run (Table 1). The shortest median ADP of low standard error in conjunction with a median very low VPD (one-quarter of the next lowest cluster) shows cluster 3 represents rain pulses occurring after initial pulses, during the wettest and windiest portion of discrete storm events (Table 1). Rain pulses in cluster 4 are of moderate magnitude, windiness, and VPD compared to the other clusters, yet these pulses' elevated variability in rainfall intensity ranks second-highest (Table 1). Median ADP being at nearly 10 h confirms that cluster 4 rain pulses include those occurring at the

HESSD
11, 11335–11368, 2014

start of discrete storm events (ADP ≥ 8 h) of very short preceding dry periods (Table 1). The standard error of ADP for cluster 4 is high enough (±8.5 h), however, to show that cluster 4 also contains intrastorm rainfall pulses under moderate windiness and atmospheric dryness that occur after a discrete storm's initial pulse (Table 1).

3.2 Throughfall generation from rainfall pulse clusters

Total throughfall produced by all rain pulses was 405.3 mm, totalling 73 % of the rainfall analysed in this study (Table 2). Median throughfall expressed as a percentage of all rainfall pulses was roughly equivalent (Table 2). CV of throughfall intensity across all rain pulses was generally higher than the median throughfall intensity (Table 2). Sums of throughfall generation per rain pulse cluster mirrored the trends seen for the total rainfall from the pulse clusters themselves: with the greatest overall throughfall depth measured from cluster 3's low VPD, windy, internal storm pulses and the lowest under cluster 1's high VPD initial storm pulses of low and steady rain intensity conditions (Table 2). No statistically significant differences were observed in the response of throughfall intensity to differing rainfall pulse clusters, as median intensities (and their standard error) were relatively low (Table 2). However, interestingly, the atmospherically drier rainfall pulses (clusters 1 and 2) generally produced greater median throughfall intensities, despite significantly lower throughfall percentages compared to the atmospherically wetter rain pulse clusters (3 and 4): $H = 20.08$, $p < 0.001$ (Table 2). As expected, median throughfall percent diminished proportionally as rain pulse clusters' increase in median VPD and ADP (Tables 1–2). Median CV of throughfall intensity only significantly differed between internal rain pulse clusters 2 and 3 ($H = 11.36$, $p < 0.01$; Table 2), which are of contrasting median atmospheric water demand (169.8 vs. 26.9 Pa VPD), windiness (18.5 vs. 76.5 km wind run), and intensity intermittency (1.1 vs. 0.6 CV in mm $(5\,\text{min})^{-1}$), respectively (Table 1). Greater intermittency of throughfall intensity for rainfall pulse cluster 2 may be a function on interacting wind-VPD conditions, as cluster 2 exhibited greater median VPD and lower median wind run compared to cluster 3 (Table 2).

HESSD
11, 11335–11368, 2014

J. T. Van Stan and T. E. Gay

Examples of data from clusters representing pulses that begin discrete storm events (clusters 1 and part of cluster 4), including meteorological conditions and their throughfall response, show distinct differences in intrastorm VPD and wind speed dynamics (Fig. 2a and b). Declining VPD introduces both starting rainfall pulses, yet for pulses in cluster 1 (where VPD and wind speeds are high) the throughfall response was relatively muted (Fig. 2a). The start-of-storm example rain pulse for cluster 4, however, produced a more reactive throughfall response under diminished VPD and wind speed conditions (Fig. 2b). Example throughfall responses to rain pulses internal to discrete storm events (clusters 2, 3 and some pulses of 4) are provided in Fig. 3a–c. The most notable difference among these internal rainfall pulses and their throughfall response is in relation to intrastorm VPD conditions, with the driest atmospheric conditions for cluster 2 (Fig. 3a), moderate conditions for cluster 4's internal pulses (Fig. 3b), and wet atmospheric conditions for cluster 3 (Fig. 3c).

3.3 MCA results: temporal hot moments in throughfall generation

Significant eigenvalues for two dimensions were found for a MCA analyzing all 69 rain-throughfall pulses, accounting for 61 % of the statistical inertia (Fig. 4). Sign and proximity of points on each dimension show degree of correspondence between the selected storm conditions and throughfall generation ≥ 80 % (TF80:1) or < 80 % (TF80:0) (Fig. 4). Just as in similar multivariate analyses (e.g., Principal Components Analysis), proximity and sign must be considered for each MCA dimension individually as they are orthogonal and, therefore, do not correspond to each other. Thus, the zero-axis for dimension 1 is a solid line; whereas this axis for dimension 2 is dashed (Fig. 4). Dimension 1 of the MCA map that includes all rain-throughfall pulses shows a grouping of TF80:1 with other points of positive sign (Fig. 4). These points represent interacting meteorological conditions corresponding to the majority of pulses where throughfall production was ≥ 80 % of precipitation (TF80:1 hot moments). Dimension 1 positive meteorological conditions indicate rain pulses producing TF80:1 hot moments have high wind-related droplet inclination ≥ 17° (A:1) under consistent winds that vary less than 0.6 m s^{-1} per 5 min period (CVW:0) with intrastorm rainfall intensities ≥ 0.6 mm 5 min^{-1} (I:1) that vary by ≥ 1 mm 5 min^{1} (CVI:1) (Fig. 4). Thus, the majority of TF80:1 hot moments for all pulses correspond to rain pulses of consistent wind-driven, inclined rainfall under high, but also highly variable, intensities (Fig. 4). The second dimension of Fig. 4 shows another significant correspondence of TF80:1 hot moments with a second mixture of meteorological conditions, also in the positive domain. Meteorological conditions corresponding to TF80:1 hot moments on the second dimension include highly variable winds ≥ 0.6 m s^{-1} per 5 min period (CVW:1) that generally do not incline rainfall ≥ 17° (A:0), with rainfall intensity ≥ 0.6 mm 5 min^{-1} (I:1) that, like dimension 1's grouping, is variable ≥ 1 mm 5 min^{1} (CVI:1) (Fig. 4). Therefore, in addition to the rain pulses identified in dimension 1, TF80:1 hot moments may correspond to non-inclined rainfall under intermittent wind conditions (Fig. 4). Regardless of dimensional differences in wind conditions and inclination angle, rain pulses of high and variable intensity consistently corresponds to TF80:1 hot moments for this canopy. Intuitively, rain pulses producing TF80:0 (< 80 % of rainfall) occur during the opposite conditions as shown by the grouping of points in the negative domains of both dimensions (Fig. 4).

To ascertain which of the pulse cluster types contribute most to these two storm condition types conducive to TF80:1 hot moments (sustained wind-driven inclined rain vs. intermittent winds with non-inclined rain), MCAs were applied to the atmospherically dry (clusters 1 and 2; Fig. 5a), wet (cluster 3; Fig. 5b) and intermediate (cluster 4; Fig. 5c) intrastorm rain pulses. Dry pulses (clusters 1 and 2), whether at the beginning of, or internal to, a storm, show a significant correspondence between TF80:1 hot moments and the Fig. 4, dimension 1 storm conditions – A:1, CVW:0, I:1, and CVI:1 – by grouping in the negative domain (Fig. 5a). Occurrence of TF80:1 hot moments under low VPD conditions (cluster 3), alternatively, grouped with the Fig. 4, dimension 2 type storm conditions in the negative domain (without correspondence with highly variable rain intensity – CVI:1) (Fig. 5b). For rain pulses under moderate atmospheric moisture demand (cluster 4), TF80:1 hot moments showed the greatest percent of the MCA *Chi*-square, corresponding very strongly with Fig. 4, dimension 1 type storm conditions, yet in the positive domain (Fig. 5c). Since three of the four pulse clusters' TF80:1 correspond most strongly with Fig. 4, dimension 1 storm conditions, it is not surprising that Fig. 4 dimension 1 represents the greater percent inertia for all storms (Fig. 4). Interestingly, the order of the closest corresponding meteorological condition thresholds to TF80:1 varied for dry vs. moderate VPD rain pulses: where intensity thresholds (I:1 and CVI:1) were closer to TF80:1 under drier VPD conditions (Fig. 5a), and variability, particularly wind, thresholds (CVW:0 and CVI:1) were closer under moderate VPD conditions (Fig. 5c). Groupings of meteorological conditions with TF80:1 hot moments are tightest for moderate VPD rain pulses (cluster 4; Fig. 5c), followed by those with low VPD (cluster 3; Fig. 5b), then, loosest for those with high VPD (clusters 1 and 2, Fig. 5a). Percent explained inertia for each MCA map also followed this trend (Fig. 5a–c). Correspondences with TF80:0 events for each of these pulse-specific MCAs grouped with the opposite meteorological conditions, as expected for this method (Fig. 5a–c).

4 Discussion

Throughfall dynamics in a variety of forest settings have been examined with respect to meteorological conditions at the interstorm and (more rarely) intrastorm scale (Levia et al., 2011), yet recent work has shown that many ecohydrological processes occur under fine-scale temporal biogeochemical and transport-driven hot moments (McClain et al., 2003; Vidon et al., 2010; Andrews et al., 2011; Liengaard et al., 2014). Still, the authors are unaware of any previous work characterizing intrastorm rainfall pulse types (i.e., Table 1), relating these rain pulse types to their throughfall response (as shown in Table 2 and Figs. 2–3), and identifying interacting meteorological conditions under which throughfall can be momentarily enhanced (like those in Figs. 4–5). This is surprising since throughfall, as a transport-driven hot moment, brings critical moisture and dissolved solute supplies to the litter and soil which could, in turn, disproportionately enhance biogeochemical processes (Levia and Frost, 2006;

HESSD
11, 11335–11368, 2014

Rain pulse influence over throughfall hot moments

J. T. Van Stan and T. E. Gay

Andrews et al., 2011; Singh et al., 2014). The inverse relationship between median throughfall percentages and VPD across the intrastorm rain pulse clusters (Tables 1–2) agrees with previous work across temporal scales, as drier atmospheric conditions likely evaporate splash and intercepted rain droplets which would have otherwise become throughfall (Llorens et al., 1997; Staelens et al., 2008; Mair and Fares, 2010). High windiness associated with the atmospherically wettest rain pulse (cluster 3, Fig. 3c) no doubt enhanced droplet capture and routing through the canopy, or through shaking-off entrained droplets (Hörmann et al., 1996; Nanko et al., 2006; Mair and Fares, 2010; Kato et al., 2013).

Meteorological factors corresponding with TF80:1 hot moments at this site for all pulses and both MCA dimensions in Fig. 4 were high intensity (I:1) with a large CV (CVI:1). Direct relationships between rain intensity and throughfall intensity have been reported by past literature (e.g., Bryant et al., 2005; Sraj et al., 2008; Kato et al., 2013), however the determination of a threshold over which more rain is typically translated into throughfall has not, to our knowledge, been reported. Note that threshold values found in this study may not be applicable to other locations, as threshold intensities where throughfall hot moments are more likely, for example, may be canopy structure dependent (just as Nanko et al. (2006) observed that throughfall droplet size distribution – which is related to intensity – can vary as a function of leaf form). A rain pulse of large CVI in conjunction with high median rain intensity may overflow throughfall pathways and, perhaps a large boost in rain intensity could even allow this overflow to bypass storage on new surfaces. Such a bypass event would diminish not only storage (compared to throughfall generation), but evaporative losses as the canopy and trunk storage supplying evaporation would be reduced. The ability for canopy water storage to be reduced under high rainfall intensities (and thus, large rain-drops) has been debated during development of a variable-storage capacity parameter for the reformulated Gash interception model (Valente et al., 1997; Price and Carlyle-Moses, 2003; Carlyle-Moses, 2004; Keim, 2004), yet the authors are unaware whether a broadly-accepted mechanism has been described

HESSD
11, 11335–11368, 2014

(latest discussion in Levia et al., 2011). Beyond the shared rain intensity characteristics for the "all pulses" MCA plot, storms of the highest correspondence with TF80:1 hot moments (Fig. 4, dimension 1) reached or exceeded a wind-driven rainfall inclination angle threshold (A:1) under steady (low CV wind speed) wind conditions. Rain pulse conditions under Fig. 4, dimension 2 did not require high rainfall inclination angles (A:0) to produce a corresponding TF80:1 hot moment, as the wind speed's high CV may create enough stops-and-starts to allow substantial rain intensities to load the canopy with entrained droplets, ripe for vibrational detachment when wind does start. Both of these mechanisms of throughfall enhancement – (dimension 1) increased wetting due to strong, consistent windy conditions inclining rainfall/breaking-up droplets, and (dimension 2) canopy vibrational release of entrained droplets – have been discussed or observed in previous work (Hörmann et al., 1996; Nanko et al., 2006; Mair and Fares, 2010; Kato et al., 2013).

Threshold meteorological conditions correspondent to TF80:1 hot moments differed across the rainfall pulse types identified by the cluster analysis (Fig. 5). Under dry to moderate VPD (Fig. 5a and c), rainfall pulses corresponded to TF80:1 hot moments during meteorological conditions similar to those discussed above regarding Fig. 4, dimension 1. Yet, strength of correspondence and order of the closest corresponding meteorological thresholds varied between rain pulse (1) intensity characteristics (median and CV of intensity) corresponding most strongly to TF80:1 hot moments under drier atmospheric conditions (Fig. 5a), and (2) low variability of wind and then high variability of intensity for more moderate atmospheric water demands (Fig. 5c). Weaker correspondences between TF80:1 and meteorological condition thresholds under higher VPD could be a result of other corresponding variables not included, like canopy structural variables as they tend to drive rainfall partitioning when able to more rapidly store, distribute and evaporate intercepted droplets (Crockford and Richardson, 2000; Marin et al., 2000; Dietz et al., 2006; Oyarzún et al., 2011). Thus, the rainfall intensity threshold would, logically, plot closest to TF80:1 in the MCA plot for rain pulses of higher VPD (Fig. 5a) as it would be the strongest driver in developing throughfall generation by overcoming canopy structural storage/evaporation controls over throughfall proportions (e.g., Price and Carlyle-Moses, 2003; Link et al., 2004; André et al., 2011). When VPD constraints are more moderate during rainfall pulses, meteorological thresholds such as consistent wind (CVW:0) sustaining high rainfall inclination angles (A:1) under variable intensity (CVI:1) plot closer to TF80:1, becoming more critical to the enhanced translation of rain into throughfall (Fig. 5c). Alternatively, under the wettest VPD conditions (Fig. 5b), consistently high wind speeds (CVW:0) inclining rainfall (A:1) corresponds very closely in the MCA map with the absence of throughfall hot moments (TF80:0). Low VPD conditions conducive to high throughfall percentages correspond strongest with inconsistent wind conditions (CVW:1) – of course, inconjunction with steady, high rain pulse intensity (Fig. 5b, CVI:0 and I:1). Correspondence of TF80:1 hot moments with erratic wind conditions and low rainfall inclination angle may seem counter-intuitive; however, it stands to reason that consistent wind inclining rainfall may actually reduce droplet detachment (to form throughfall) as a result of two mechanisms: (1) consistent wind can break rainfall into finer droplets which are more easily evaporated; and (2) which saturate greater canopy surface area, increasing water storage available to evaporation (Calder, 1996; Nanko et al., 2004, 2006; Murakami, 2006). Further, when the atmosphere has a low water vapour demand (as for the MCA map in Fig. 5b), wind can play a more significant role in facilitating evaporation (Penman, 1948; Priestly and Taylor, 1972).

Efforts to characterize the influence of interacting meteorological conditions on throughfall have been few, and primarily limited to stepwise regression (e.g., Staelens et al., 2008; André et al., 2011) and analytical models (e.g., Rutter et al., 1971; Calder, 1977; Valente et al., 1997; Keim and Skaugset, 2004; Trinh and Chui, 2013). To the knowledge of the authors, none of these have been applied to identify a mixture of threshold meteorological conditions under which throughfall may be preferentially enhanced (as is possible with MCA and demonstrated in Figs. 4–5). The MCA methodology described here can be applied across a range of conditions at other sites, provided the hydrometeorological data is available at the desired temporal

Discussion Paper | Discussion Paper | Discussion Paper | Discussion Paper |

HESSD
11, 11335–11368, 2014

Rain pulse influence over throughfall hot moments

J. T. Van Stan and T. E. Gay

resolution. This may enable cross-site comparisons of differing forest structure (e.g., with and without heavy epiphyte cover) control over meteorological thresholds conducive to enhanced translation of rain into throughfall. Perhaps the cocktail of meteorological condition thresholds corresponding to throughfall hot moments in this maritime subtropical *Q. virginiana* forest is, in no small part, a function of the heavy *T. usneoides* coverage. Several studies have shown that epiphyte biomass, despite having a large potential canopy water storage, oftentimes are not sufficiently dry in situ to significantly enhance interception losses (Hölscher et al., 2004; Pypker et al., 2006a; Van Stan et al., 2014). As *T. usneoides* grows in a pendulous form, primarily drooping from branch confluences toward the surface, its structure (when saturated) may be the primary interaction with these threshold meteorological conditions to promote preferential throughfall drainage. Similar mechanisms for spatially-enhanced throughfall production have been discussed by others in the tropics (e.g., Zimmermann et al., 2007). Where throughfall drainage pathways depend on other canopy structures (leaves, twigs, branches, etc.), meteorological interactions and condition thresholds may differ with regards to adequately preparing those elements for throughfall hot moments within storms.

5 Conclusions

This study has identified intrastorm rainfall pulse clusters of distinct meteorological conditions, characterized their influences over throughfall responses, and applied MCA to identify corresponding threshold meteorological conditions under which translation of rainfall into throughfall was enhanced (TF80:1 hot moments) for an epiphyte-laden maritime *Q. virginiana* canopy. Primary meteorological thresholds corresponding with TF80:1 hot moments across all rain pulse types were, intuitively, intensity variables (high median and CV of 5 min rainfall intensity). Conditions on either side of the wind-driven rainfall inclination angle and CV wind speed thresholds – in conjunction with high intensity thresholds – corresponded with TF80:1 hot moments potentially

HESSD
11, 11335–11368, 2014

J. T. Van Stan and T. E. Gay

as a result of two differing wind-induced throughfall enhancement mechanisms: (1) increased surface wetting for high wind-driven rainfall inclination angles under steady (low CV wind speed) wind conditions (MCA map dimension 1); and (2) sporadic start-stop wind conditions shaking droplets from surfaces – a process where inclination angle is not entirely necessary. These correspondences were strongest (greatest % inertia) during rain pulses of moderate VPD, and weakest under drier atmospheric moisture conditions. Moderate VPD constraints during rainfall pulses of consistent wind sustaining high rainfall inclination angles under variable intensity corresponded strongest to TF80:1 hot moments. Atmospherically wet rain pulse conditions, however, corresponded strongest with erratic wind speeds during steady, high intensities. Weaker correspondences between TF80:1 hot moments and meteorological condition thresholds for high VPD rain pulses may be due to canopy structural variable controls not included in the MCA. Thus, we recommend that future research couple canopy structural thresholds (branch angle, bark thicknesses/roughness, leaf area index, epiphyte load, etc.) with meteorological thresholds to identify interacting controls over throughfall hot moments under high VPD conditions. Meteorological condition thresholds producing the strongest correspondences to TF80:1 hot moments at St. Catherine's Island may be a function of heavy *T. usneoides* coverage. Throughfall drainage pathways in other locations may depend on different structures (leaves, twigs, branches, etc.), suggesting that future applications of MCA within other forest stands are needed to characterize how meteorological condition thresholds and correspondences with moments of enhanced throughfall may be affected by differing canopy characteristics. Canopy structural variability across sites also calls for caution when applying threshold values found in this study to other locations.

Acknowledgements. The authors gratefully acknowledge Royce Hayes, Mike Halderson, and the staff at the St. Catherine's Island Foundation for supporting infrastructure and access. We also thank Elliott Lewis, Brett Jenkins, Dean Moore, and Josh Schrom for their assistance in site maintenance tasks (including, but certainly not limited to, wild hog control).

HESSD
11, 11335–11368, 2014

J. T. Van Stan and T. E. Gay

Title Page
Abstract | Introduction
Conclusions | References
Tables | Figures
◂◂ | ▸▸
◂ | ▸
Back | Close
Full Screen / Esc
Printer-friendly Version
Interactive Discussion

References

André, F., Jonard, M., and Ponette, Q.: Influence of species and rain event characteristics on stemflow volume in a temperate mixed oak-beech stand, Hydrol. Process., 22, 4455–4466, 2008.

André, F., Jonard, M., Jonard, F., and Ponette, Q.: Spatial and temporal patterns of throughfall volume in a deciduous mixed-species stand, J. Hydrol., 400, 244–254, 2011.

Andrews, D. M., Lin, H., Zhu, Q., Jin, L., and Brantley, S. L.: Hot spots and hot moments of dissolved organic carbon export and soil organic carbon storage in the Shale Hills catchment, Vadose Zone J., 10, 943–954, 2011.

Bachmair, S. and Weiler, M.: New dimensions of hillslope hydrology, in: Forest Hydrology and Biogeochemistry: Synthesis of Past Research and Future Directions, Ecological Studies Series No. 216, chap. 23, Springer-Verlag, Heidelberg, Germany, 740 pp., 2011.

Bryant, M. L., Bhat, S., and Jacobs, J. M.: Measurements and modelling of throughfall variability for five forest communities in the southeastern US, J. Hydrol., 312, 95–108, 2005.

Bundt, M., Widmer, F., Pesaro, M., Zeyer, J., and Blaser, P.: Preferential flow paths: biological "hot spots" in soils, Soil Biol. Biochem., 33, 729–738, 2001.

Calder, I. R.: A model of transpiration and interception loss from a spruce forest in Plynlimon, Central Wales, J. Hydrol., 33, 247–265, 1977.

Calder, I. R.: Dependence of rainfall interception on drop size 1. Further development of the stochastic model, J. Hydrol., 185, 363–378, 1996.

Carlyle-Moses, D. E.: A reply to R. Keim's comment on "Measurement and modelling of growing-season canopy water fluxes in a mature mixed deciduous forest stand, southern Ontario, Canada", Agr. Forest Meteorol., 124, 281–284, 2004.

Carlyle-Moses, D. E. and Gash, J. H. C.: Rainfall interception loss by forest canopies, in: Forest Hydrology and Biogeochemistry: Synthesis of Past Research and Future Directions, Ecological Studies Series No. 216, chap. 20, Springer-Verlag, Heidelberg, Germany, 740 pp., 2011.

Chaves, J., Neill, C., Germer, S., Neto, S. G., Krusche, A., and Elsenbeer, H.: Land management impacts on runoff sources in small Amazon watersheds, Hydrol. Process., 22, 1766–1775, 2008.

HESSD

11, 11335–11368, 2014

Rain pulse influence over throughfall hot moments

J. T. Van Stan and T. E. Gay

Crockford, R. H. and Richardson, D. P.: Partitioning of rainfall into throughfall, stemflow and interception: effect of forest type, ground cover and climate, Hydrol. Process., 14, 2903–2920, 2000.

Dietz, J., Hölscher, D., Leuschner, C., and Hendrayanto: Rainfall partitioning in relation to forest canopy structure in differently managed montane forest stands in Central Sulawesi, Indonesia, Forest Ecol. Manag., 237, 170–178, 2006.

Fathizadeh, O., Attarod, P., Keim, R. F., Stein, A., Amiri, G. Z., and Darvishsefat, A. A.: Spatial heterogeneity and temporal stability of throughfall under individual *Quercus brantii* trees, Hydrol. Process., 28, 1124–1136, 2014.

GA-DNR-WRD (Georgia Department of Natural Resources, Wildlife Resources Division), available at: http://www.georgiawildlife.com/node/1060 (last access: 13 September 2013), 2013.

GA Office of the State Climatologist, available at: http://www.gaepd.org/Documents/stateclimatology.html last access: 13 September 2013, 2012.

Gunn, R. and Kinzer, G. D.: The terminal velocity of fall for water droplets in stagnant air, J. Meteorol., 6, 243–248, 1949.

Guswa, A. J. and Spence, C. M.: Effect of throughfall variability on recharge: application to hemlock and deciduous forests in western Massachusetts, Ecohydrology, 5, 563–574, 2012.

Hall, L. R.: Interception loss as a function of rainfall and forest types: stochastic modelling for tropical canopies revised, J. Hydrol., 280, 1–12, 2003.

Helvey, J. D. and Patric, J. H.: Canopy and litter interception of rainfall by hardwoods of eastern United States, Water Resour. Res., 1, 193–206, 1965.

Herwitz, S. R.: Interception storage capacities of tropical rainforest canopy trees, J. Hydrol., 77, 237–252, 1985.

Herwitz, S. R.: Raindrop impact and water flow on the vegetative surfaces of trees and the effects on stemflow and throughfall generation, Earth Surf. Proc. Land., 12, 425–432, 1987.

Herwitz, S. R. and Slye, R. E.: Spatial variability in the interception of inclined rainfall by a tropical rainforest canopy, Selbyana, 13, 62–71, 1992.

Herwitz, S. R. and Slye, R. E.: Three-dimensional modelling of canopy tree interception of wind-driven rainfall, J. Hydrol., 168, 205–226, 1995.

Holder, C. D.: Effects of leaf hydrophobicity and water droplet retention on canopy storage capacity, Ecohydrol., 6, 483–490, 2013.

Hölscher, D., Köhler, L., van Dijk, A. I. J. M., and Bruijnzeel, L. A.: The importance of epiphytes to total rainfall interception by a tropical montane rain forest in Costa Rica, J. Hydrol., 292, 308–322, 2004.
Hörmann, G., Branding, A., Clemen, T., Herbst, M., Hinrichs, A., and Thamm, F.: Calculation and simulation of wind controlled canopy interception of a beech forest in Northern Germany, Agr. Forest Meteorol., 79, 131–148, 1996.
Horton, R. E.: Rainfall interception, Mon. Weather Rev., U7, 603–623, 1919.
Husk, G. J., Weishampel, J. F., and Schlesinger, W. H.: Mineral dynamics in Spanish moss, *Tillandsia usneoides* L. (Bromeliaceae) from central Florida, USA, Sci. Total Environ., 321, 165–172, 2004.
Inamdar, S. P. and Mitchell, M. J.: Storm event exports of dissolved organic nitrogen (DON) across multiple catchments in a glaciated forest watershed, J. Geophys. Res., 112, G02014, doi:10.1029/2006JG000309, 2007.
James, A. L. and Roulet, N. T.: Investigating the applicability of end member mixing analysis (EMMA) across scale: a study of eight small, nested catchments in a temperate forested watershed, Water Resour. Res., 42, W08434, doi:10.1029/2005WR004419, 2006.
Kato, H., Onda, Y., Nanko, K., Gomi, T., Yamanaka, T., and Kawaguchi, S.: Effect of canopy interception on spatial variability and isotopic composition of throughfall in Japanese cypress plantations, J. Hydrol., 504, 1–11, 2013.
Keim, R. F.: Comment on "Measurement and modelling of growing-season canopy water fluxes in a mature mixed deciduous forest stand, southern Ontario, Canada", Agr. Forest Meteorol., 124, 277–279, 2004.
Keim, R. F. and Skaugset, A. E.: A linear system model of dynamic throughfall rates beneath forest canopies, Water Resour. Res., 40, W05208, doi:10.1029/2003WR002875, 2004.
Keim, R.F., Skaugset, A.E., Link, T.E., and Iroumé, A.: A stochastic model of throughfall for extreme events, Hydrol. Earth Syst. Sci., 8, 23–34, doi:10.5194/hess-8-23-2004, 2004.
Keim, R. F., Skaugset, A. E., and Weiler, M.: Temporal persistence of spatial patterns in throughfall, J. Hydrol., 314, 263–274, 2005.
Keim, R. F., Skaugset, A. E., and Weiler, M.: Storage of water on vegetation under simulated rainfall of varying intensity, Adv. Water Resour., 29, 974–986, 2006.
Köhler, L., Tobfin, C., Frumau, K. F. A., and Bruijnzeel, L. A.: Biomass and water storage dynamics of epiphytes in old-growth and secondary montane cloud forest stands in Costa Rica, Plant Ecol., 193, 171–184, 2007.

HESSD
11, 11335–11368, 2014

Rain pulse influence over throughfall hot moments

J. T. Van Stan and T. E. Gay

Kumagai, T- O.: Transpiration in forest ecosystems, in: Forest Hydrology and Biogeochemistry: Synthesis of Past Research and Future Directions, Ecological Studies Series No. 216, Springer-Verlag, Heidelberg, Germany, chap. 19, 740 pp., 2011.

Laws, J. O. and Parsons, D. A.: The relation of raindrop-size to intensity, T. Am. Geophys. Un., 2, 452–460, 1943.

Leingaard, L., Figueiredo, V., Markfoged, R., Revsbech, N. P., Nielsen, L. P., Prast, A. E., and Kühl, M.: Hot moments of N_2O transformation and emission in tropical soils from the Pantanal and the Amazon (Brazil), Soil Biol. Biochem., 75, 26–36, 2014.

Levia, D. F. and Frost, E. E.: Variability of throughfall volume and solute inputs in wooded ecosystems, Prog. Phys. Geog., 30, 605–632, 2006.

Levia, D. F., Keim, R. F., Carlyle-Moses, D. E., and Frost, E. E.: Throughfall and stemflow in wooded ecosystems, in: Forest Hydrology and Biogeochemistry: Synthesis of Past Research and Future Directions, Ecological Studies Series No. 216, chap. 21, Springer-Verlag, Heidelberg, Germany, 740 pp., 2011.

Link, T. E., Unsworth, M., and Marks, D.: The dynamics of rainfall interception by a seasonal temperate rainforest, Agr. Forest Meteorol., 124, 171–191, 2004.

Llorens, P., Poch, R., Latron, J., and Gallart, F.: Rainfall interception by a *Pinus sylvestris* forest patch overgrown in a Mediterranean mountainous abandoned area I. Monitoring design and results down to the event scale, J. Hydrol., 199, 331–345, 1997.

Mair, A. and Fares, A.: Throughfall characteristics in three non-native Hawaiian forest stands, Agr. Forest Meteorol., 150, 1453–1466, 2010.

Manderscheid, B. and Matzner, E.: Spatial and temporal variation of soil solution chemistry and ion fluxes through the soil in a mature Norway spruce (*Picea abies* (L.) Karst.) stand, Biogeochemistry, 30, 99–114, 1995.

Marin, C. T., Bouten, W., and Sevink, J.: Gross rainfall and its partitioning into throughfall, stemflow, and evaporation of intercepted water in four forest ecosystems in western Amazonia, J. Hydrol., 237, 40–57, 2000.

McClain, M. E., Boyer, E. W., Dent, L., Gergel, S. E., Grimm, N. B., Groffman, P. M., Hart, S. C., Harvey, J. W., Johnston, C. A., Mayorag, W., McDowell, W. H., and Pinay, G.: Biogeochemical hot spots and hot moments at the interface of terrestrial and aquatic ecosystems, Ecosystems, 6, 301–312, 2003.

Murakami, S.: A proposal for a new forest canopy interception mechanism: splash droplet evaporation, J. Hydrol., 319, 72–82, 2006.

HESSD
11, 11335–11368, 2014

Rain pulse influence over throughfall hot moments

J. T. Van Stan and T. E. Gay

Nanko, K., Hotta, N., and Suzuki, M.: Assessing raindrop impact energy at the forest floor in a mature Japanese cypress plantation using continuous raindrop-sizing instruments, J. For. Res.-Jpn., 9, 157–164, 2004.
Nanko, K., Hotta, N.,and Suzuki, M.: Evaluating the influence of canopy species and meteorological factors on throughfall drop size distribution, J. Hydrol., 329, 422–431, 2006.
Návar, J. and Bryan, R.: Interception loss and rainfall redistribution by three semi-arid growing shrubs in northeastern Mexico, J. Hydrol., 115, 51–63, 1990.
Oyarzún, C. E., Godoy, R., Staelens, J., Donoso, P. J., and Verhoest, N. E. C.: Seasonal and annual throughfall and stemflow in Andean temperate rainforests, Hydrol. Process., 25, 623–633, 2011.
Penman, H. L.: Natural evaporation from open water, bare soil and grass, P. Roy. Soc. Lond. A Mat., 193, 120–145, 1948.
Preisendorfer, R. W., Zweirs, F. W., and Barnett, T. P.: Principal Component Selection Rules, Scripps Institute of Oceanography, SIO Ref. Ser. 81-4, La Jolla, CA, USA, 200 pp., 1981.
Price, A. G. and Carlyle-Moses, D. E.: Measurement and modelling of growing-season canopy water fluxes in a mature mixed deciduous forest stand, southern Ontario, Canada, Agr. Forest Meteorol., 119, 69–85, 2003.
Priestly, C. H. B. and Taylor, R. J.: On the assessment of surface heat flux and evaporation using large-scale parameters, Mon. Weather Rev., 100, 81–92, 1972.
Pypker, T. G., Unsworth, M. H., and Bond, B. J.: The role of epiphytes in rainfall interception by forests in the Pacific Northwest. I. Laboratory measurements of water storage, Can. J. Forest Res., 36, 809–818, 2006a.
Pypker, T. G., Unsworth, M. H., and Bond, B. J.: The role of epiphytes in rainfall interception by forests in the Pacific Northwest, II. Field measurements at the branch and canopy scale, Can. J. Forest Res., 36, 819–832, 2006b.
Pypker, T. G., Levia, D. F., Staelens, J., and Van Stan, J. T.: Canopy structure in relation to hydrological and biogeochemical fluxes, in: Forest Hydrology and Biogeochemistry: Synthesis of Past Research and Future Directions, Ecological Studies Series No. 216, chap. 18, Springer-Verlag, Heidelberg, Germany, 740 pp., 2011.
Rosado, B. H. P. and Holder, C. D.: The significance of leaf water repellency in ecohydrological research: a review, Ecohydrology, 6, 150–161, 2013.

HESSD
11, 11335–11368, 2014

Rain pulse influence over throughfall hot moments

J. T. Van Stan and T. E. Gay

Rutter, A. J., Kershaw, K. A., Robins, P. C., and Morton, A. J.: A predictive model of rainfall interception in forests, I. Derivation of the model from observations in a plantation of Corsican pine, Agr. Meteorol., 9, 367–376, 1971.

Schlesinger, W. H. and Marks, P. L.: Mineral cycling and the niche of Spanish moss, *Tillandsia usneoides* L., Am. J. Bot., 64, 1254–1262, 1977.

Shachnovich, Y., Berliner, P. R., and Bar, P.: Rainfall interception and spatial distribution of throughfall in a pine forest planted in an arid zone, J. Hydrol., 349, 168–177, 2008.

Singh, S., Inamdar, S. P., Mitchell, M. J., and McHale, P.: Seasonal pattern of dissolved organic matter (DOM) in watershed sources: influence of hydrologic flow paths and autumnal leaf fall, Biogeochemistry, 118, 321–337, 2014.

Sraj, M., Brilly, M., and Mikos, M.: Rainfall interception by two deciduous Mediterranean forests of contrasting stature in Slovenia, Agr. Forest Meteorol., 148, 121–134, 2008.

Staelens, J., De Schrijver, A., Verheyen, K., and Verhoest, N. E. C.: Rainfall partitioning into throughfall, stemflow, and interception within a single beech (*Fagus sylvatica* L.) canopy: influence of foliation, rain event characteristics, and meteorology, Hydrol. Process., 22, 33–45, 2008.

Stout, B. B. and McMahon, R. J.: Throughfall variation under tree crowns, J. Geophys. Res., 66, 1839–1843, 1961.

Tan, P- N., Steinbach, M., and Kumar, V.: Cluster analysis: basic concepts and algorithms, in: Introduction to Data Mining, chap. 8, Addison-Wesley, Boston, MA, USA, 769 pp., 2005.

Tanaka, T.: Effects of the canopy hydrologic flux on groundwater, in: Forest Hydrology and Biogeochemistry: Synthesis of Past Research and Future Directions, Ecological Studies Series No. 216, chap. 25, Springer-Verlag, Heidelberg, Germany, 740 pp., 2011.

Trinh, D. H. and Chui, T. F. M.: An empirical method for approximating canopy throughfall, Hydrol. Process., 27, 1764–1772, 2013.

Valente, F., David, J. S., and Gash, J. H. C.: Modelling interception loss for two sparse eucalypt and pine forests in central Portugal using reformulated Rutter and Gash analytical models, J. Hydrol., 190, 141–162, 1997.

Van Stan, J. T., Siegert, C. M., Levia, D. F., and Scheick, C. E.: Effects of wind-driven rainfall on stemflow generation between codominant tree species with differing crown characteristics, Agr. Forest Meteorol., 151, 1277–1286, 2011.

HESSD

11, 11335–11368, 2014

Rain pulse influence over throughfall hot moments

J. T. Van Stan and T. E. Gay

Van Stan, J. T., Stubbins, A., Bittar, T., Reichard, J. S., Wright, K. A., and Jenkins, R. B.: *Tillandsia usneoides* (L.) L. (Spanish moss) water storage and leachate characteristics from two maritime oak forest settings, Ecohydrology, in press, 2014.

Vidon, P., Allan, C., Burns, D., Duval, T. P., Gurwick, N., Inamdar, S. P., Lowrance, R., Okay, J., Scott, D., and Sebestyen, S.: Hot spots and hot moments in riparian zones: potential for improved water quality management, J. Am. Water Resour. As., 46, 278–298, 2010.

Zimmermann, A., Wilcke, W., and Elsenbeer, H.: Spatial and temporal patterns of throughfall quantity and quality in a tropical montane forest in Ecuador, J. Hydrol., 343, 80–96, 2007.

Zimmermann, A., Zimmermann, B., and Elsenbeer, H.: Rainfall redistribution in a tropical forest: spatial and temporal patterns, Water Resour. Res., 45, W11412, doi:10.1029/2008WR007470, 2009.

Table 1. Descriptive statistics for the rainfall pulse clusters identified by complete linkage cluster analysis.

Pulse Cluster	n	Median (std. error) Sum rain (mm)	Rain (mm)	CV intensity (mm (5 min)$^{-1}$)	Wind run (km)	VPD (Pa)	ADP (h)
1	11	41.7	1.5 (1.6)	0.2 (0.2)	4.0 (24.7)	349.6 (89.5)	86.7 (21.5)
2	12	108.3	2.9 (3.3)	1.1 (0.1)	18.5 (37.8)	169.8 (12.3)	4.4 (3.5)
3	29	293.2	5.1 (2.4)	0.6 (0.2)	76.5 (23.4)	26.9 (3.5)	1.4 (3.6)
4	17	109.6	2.5 (1.8)	0.8 (0.2)	16.7 (13.6)	110.5 (5.7)	9.6 (8.5)
All	69	552.8	2.7 (1.1)	0.8 (0.1)	21.0 (11.3)	94.2 (19.2)	4.0 (5.7)

HESSD
11, 11335–11368, 2014

Rain pulse influence over throughfall hot moments

J. T. Van Stan and T. E. Gay

Table 2. Throughfall pulse characteristics for each cluster identified by complete linkage cluster analysis. Superscripts indicate the order of medians (from high to low in alphabetical order) where similar superscripts indicate insignificantly different medians per Kruskal–Wallis ANOVA ($p > 0.05$).

		Median (std. error)			
Pulse Cluster	n	Sum (mm)	% Rain (%)	Intensity (mm h^{-1})	CV intensity (mm (5 min)$^{-1}$)
1	11	21.6	37 (8)^{b}	0.5 (0.3)	0.9 (0.2)^{ab}
2	12	64.3	66 (6)^{ab}	0.4 (0.4)	1.3 (0.1)^{a}
3	29	241.2	88 (3)^{a}	0.3 (0.2)	0.8 (0.1)^{b}
4	17	78.2	75 (7)^{a}	0.2 (0.3)	0.9 (0.1)^{ab}
All	69	405.3	71 (3)	0.4 (0.1)	0.9 (0.1)

HESSD
11, 11335–11368, 2014

Rain pulse influence over throughfall hot moments

J. T. Van Stan and T. E. Gay

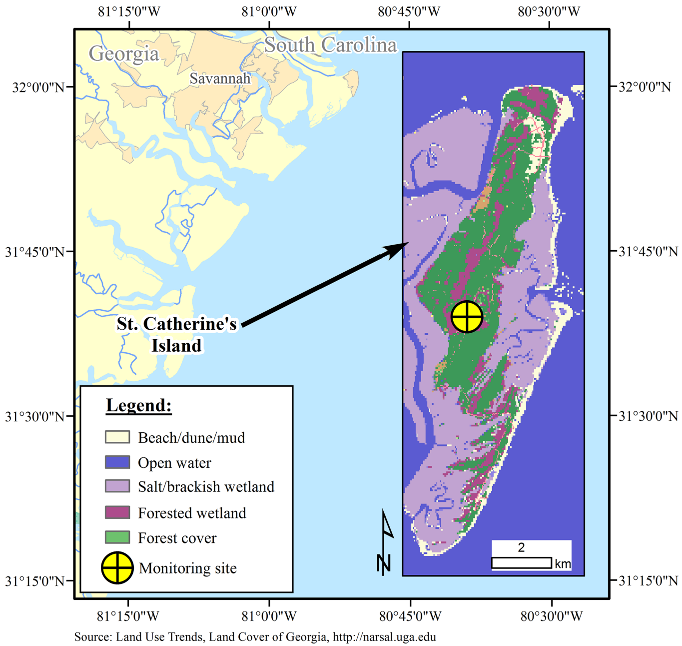

Figure 1. Location of the biometeorological monitoring site at St. Catherine's Island, Georgia, USA and surrounding land use classifications as of 2010.

HESSD
11, 11335–11368, 2014

Rain pulse influence over throughfall hot moments

J. T. Van Stan and T. E. Gay

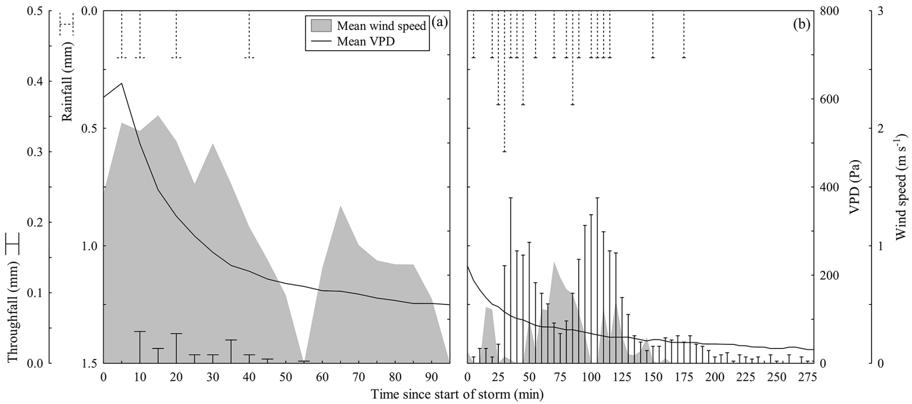

Figure 2. Example start-of-storm pulses plotted against major intrastorm meteorological factors, where **(a)** shows the archetypical "dry start" after a long ADP (cluster 1 – example pulse: 0.8 mm rainfall, 0.19 mm throughfall), vs. **(b)** a more atmospherically moist beginning with a shorter ADP (some in cluster 4 – example pulse: 4.6 mm rainfall and 3.46 mm throughfall). 5 min rainfall and throughfall intensities shown from top axis with dashed whiskers and bottom axis with solid whiskers, respectively.

HESSD
11, 11335–11368, 2014

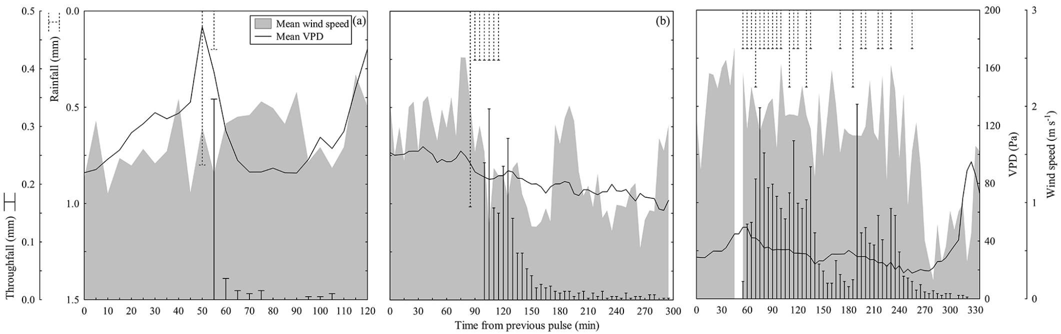

Figure 3. Interior rain-throughfall pulse examples plotted against major meteorological conditions, where time from the previous pulse is roughly equivalent, yet atmospheric conditions range from **(a)** drier (cluster 2 – example 1.0 mm rainfall, 0.45 mm throughfall), **(b)** more moderate (some in cluster 4 – example 2.5 mm rainfall, 2.0 mm throughfall), and **(c)** wetter (cluster 3 – example 5.4 mm rainfall, 5.27 mm throughfall). 5 min rainfall and throughfall intensities shown from top axis with dashed whiskers and bottom axis with solid whiskers, respectively.

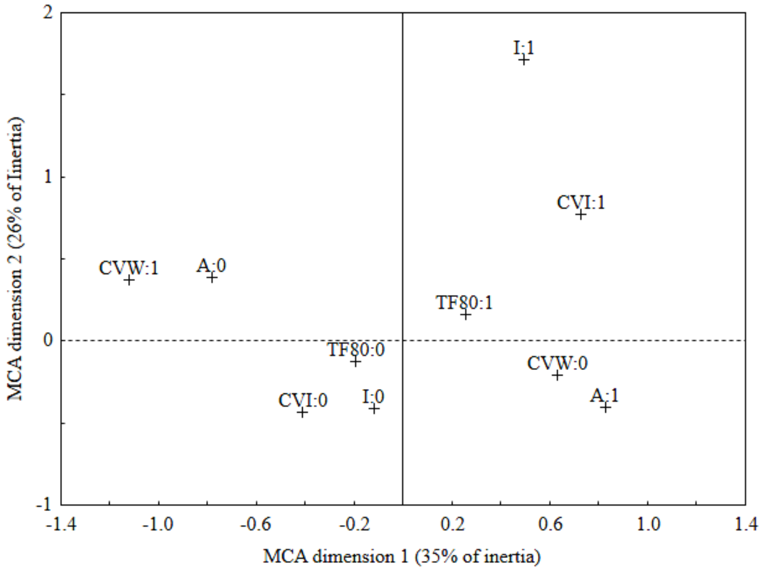

Figure 4. Two-dimensional multiple correspondence map for all 69 rain-throughfall pulses showing correspondence between throughfall generation ≥ 80 % rainfall (TF80:1), < 80 % rainfall (TF80:0), and meteorological conditions: inclination angle ≥ 17° (A:1 vs. A:0), rainfall intensity ≥ 0.6 mm 5 min^{-1} (I:1 vs. I:0), coefficient of variation in 5 min wind speed ≥ 0.6 m s^{-1} (CVW:1 vs. CVW:0), coefficient of variation in rainfall intensity ≥ 1 mm 5 min^{-1} (CVI:1 vs. CVI:0). Dimension 1 clusters fall to the left/right of the solid 0-line, whereas dimension 2 clusters are bisected top/bottom by the dashed 0-line.

HESSD
11, 11335–11368, 2014

Rain pulse influence over throughfall hot moments

J. T. Van Stan and T. E. Gay

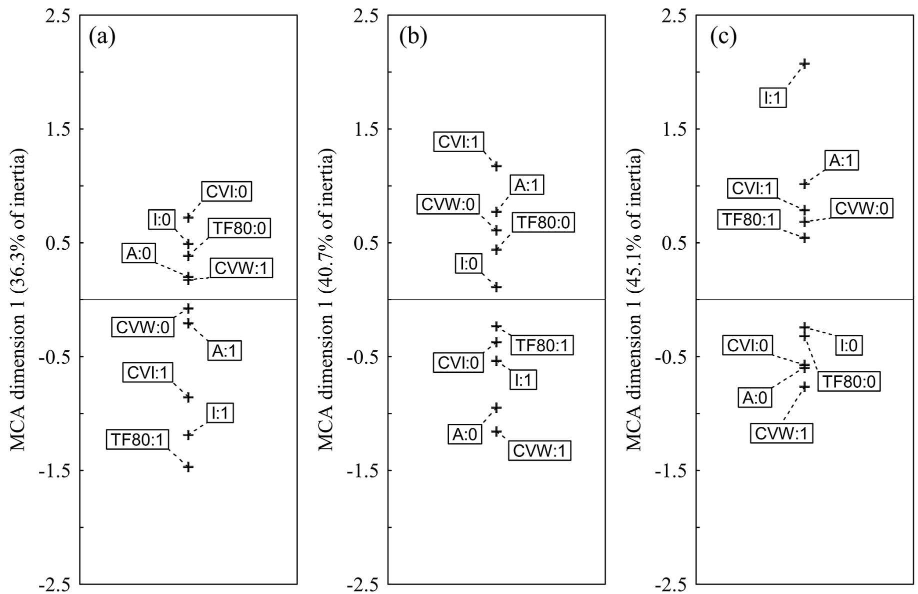

Figure 5. One-dimensional MCA maps for **(a)** atmospherically dry beginning (cluster 1) and intrastorm (cluster 2) pulses, **(b)** intrastorm atmospherically wet pulses (cluster 3), and beginning/intrastorm pulses of intermediate VPD (cluster 4). Strength of correspondence is indicated first by sign, and second by the proximity of points in the positive or negative domain.

HESSD
11, 11335–11368, 2014

Rain pulse influence over throughfall hot moments

J. T. Van Stan and T. E. Gay